17th World Conference on Earthquake Engineering, 17WCEE
Sendai, Japan - September 13th to 18th 2020

CONTRIBUTIONS TO THE DEVELOPMENT OF ELEMENTAL VISCOUS DAMPING MODELS

N. A. Clemett [1], A. J. Carr [2], A. Filiatrault [3,4]

[1] *Graduate Student, IUSS Pavia, n.clemett@meees.org*
[2] *Professor Emeritus, University of Canterbury, athol.carr@canterbury.ac.nz*
[3] *Professor, University School for Advanced Studies, IUSS Pavia, andre.filiatrault@iusspavia.it*
[4] *Professor, State University of New York at Buffalo, af36@buffalo.edu*

Abstract

The aim of this paper is to provide insight into the response of structures modelled with a new elemental viscous damping model. The elemental viscous damping model developed in this study uses the element deformation mode shapes and frequencies to construct a damping matrix for each individual beam or column element. These elemental viscous damping matrices can be used to directly calculate member damping forces or, combined using the direct stiffness method to obtain a global viscous damping matrix. In particular, this study investigates: (1) what relationship exists between the level of viscous damping specified at the element level and the observed global viscous damping ratio for single and multi-storey frames; (2) how damping assigned to different elements affects the observed global viscous damping ratio, and; (3) how variations in the beam/column stiffness affect the observed global viscous damping ratio.

Linear free vibration analysis was used to investigate the relationship between the elemental viscous damping factor and the global viscous damping ratio. Three different elemental viscous damping configurations were considered; (1) beam element viscous damping only; (2) column element viscous damping only, and; (3) beam and column viscous damping.

This study highlighted that the relationship between elemental viscous damping and the observed damping ratio is complex and is affected by a variety of different variables.

Keywords: elemental viscous damping; linear free vibration; damping models

1. Introduction

Damping is an important aspect of dynamic analyses because it attenuates the response of vibrating systems. Excluding or improperly modelling the effects of damping in the analysis of a structure can result in an unrealistic representation of a structure's behaviour. This has important implications for both the assessment of existing, and the design of new, structures.

Modern time-history dynamic analyses typically employ classical viscous damping matrices such as the Rayleigh initial stiffness [1] or modal damping matrix [2] to model the effects of damping on the structure. However, since the early 1980's, studies have shown that there are some limitations in using these viscous damping matrices in nonlinear analysis. The primary concern for most researchers is that these damping models can generate unintended damping forces as the structure yields [3-5]. It has been shown that these unintended damping forces can affect the structural displacements and the forces within the members [6,7]. Many of the studies that identify the presence of these unintended damping forces also propose methods for their mitigation. Most of these proposals attempt to retain the classical nature of the viscous damping matrix, although, this is not a requirement of the analysis process.

Recent work has focussed on the development of a new viscous damping model that is formed at the element level [8-10]. This new model directly associates viscous damping with individual structural members and their deformation modes, rather than the modes of the entire structure. This model has the potential to minimise the effects of unintended damping forces in nonlinear analyses and has other advantages, such as computational efficiency and reduction of storage space of large fully populated damping matrices. However, research has also shown that the elemental viscous damping ratios are different to the global viscous damping ratios observed in free vibration tests [10]. As this model is nonclassical by nature, more research needs to be conducted to determine how it affects the response of different structural configurations, and what link, if any, exists between the prescribed elemental viscous damping ratio and the observed global viscous damping. This is the purpose of this study. Emphasis is placed on describing the relationship between the elemental viscous damping ratio and the global viscous damping ratio for frames with different structural properties.

1.1 The elemental viscous damping model

The elemental viscous damping matrix C_e used in the present study was derived following the procedure outlined in [9] and represents the viscous damping for an axially rigid two-dimensional flexural member (Fig. 1). θ_1 and θ_2 represent the deformations of the beam element and E, I, and L are the elastic modulus, moment of inertia, and length of the element respectively.

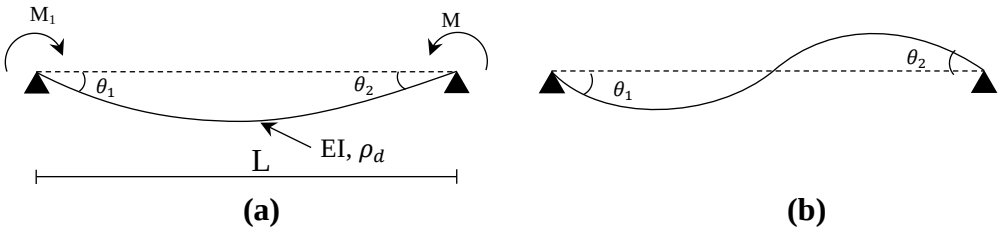

Fig. 1 – Simply supported beam mode that represents the flexural deformations of a typical beam member. (a) Mode 1 – single curvature, (b) Mode 2 – shear, double curvature.

This model assumes that damping is associated with the deformations of the structural elements. Therefore, the rigid-body motion does not produce any viscous damping. The elemental viscous damping matrix corresponding to the nodal velocities at the end of a 2D element is presented in Eq. 1. In Eq. 1, D_F is the damping factor associated in this study to the damping ratio assigned to the element expressed as a percentage. This allows the elemental viscous damping ratio to be easily distinguished from the observed viscous damping

ratio and is consistent with the input parameters of the software RUAUMOKO3D [11] used in this study. ρ_d is the damping mass assigned to the element and represents the mass that is associated with the damping member natural frequencies used to determine the viscous damping matrix. The value of the damping mass is largely arbitrary as it is effectively a scaling factor on the viscous damping actions. The damping mass values used in the present study are described in Section 2.1.

$$[C_e] = \frac{D_F}{100}\sqrt{EI\rho_d L^2}\begin{bmatrix} \frac{0.478}{L^2} & \frac{0.239}{L} & -\frac{0.478}{L^2} & -\frac{0.239}{L} \\ \frac{0.239}{L} & 0.302 & \frac{0.239}{L} & -0.062 \\ -\frac{0.478}{L^2} & \frac{0.239}{L} & \frac{0.478}{L^2} & \frac{0.239}{L} \\ -\frac{0.239}{L} & -0.062 & \frac{0.239}{L} & 0.302 \end{bmatrix} \quad (1)$$

2. Linear Free Vibration Analysis of Simple Frame Structures

2.1 Model and analysis method

The analyses were performed using a single bay, single storey frame. Linear elastic analyses were used to investigate the relationship between the damping factor, D_F, applied at the element level and the observed global viscous damping ratio, ξ. The global viscous damping ratio was estimated by observing the decay of the free vibration amplitude in simulated snapback tests. Various configurations of elemental viscous damping were investigated by applying damping to; (1) the beams only (BO), (2) the columns only (CO), and; (3) both the beams and columns (BC).

The frame used in the analysis is shown in Fig. 2. Nodes N2 and N4 are free to rotate and translate horizontally but are restrained in the vertical direction. The beam and columns were modelled using elastic beam elements and are assumed to be axially rigid. Rigid end blocks and panel zone flexibilities were not considered. Geometric P-Δ effects were not considered. The columns were modelled with the properties of a W14x311 steel section. The stiffness of the beam was varied during the analysis to investigate what effect the relative stiffness of the beams and columns has on the observed global viscous damping ratio. A range of beam to column stiffness ratios were investigated ranging from $SR = 0.4$ up to $SR = \infty$ (rigid beam).

The structural mass was modelled using RUAMOKO3D's diagonal mass formulation. The beams and columns are considered to have a distributed mass due to their self-weight (ρ_{SW} = 4.5 kN/m). The storey mass of 2000 kN was modelled as lumped mass with 1000 kN placed at nodes N2 and N4.

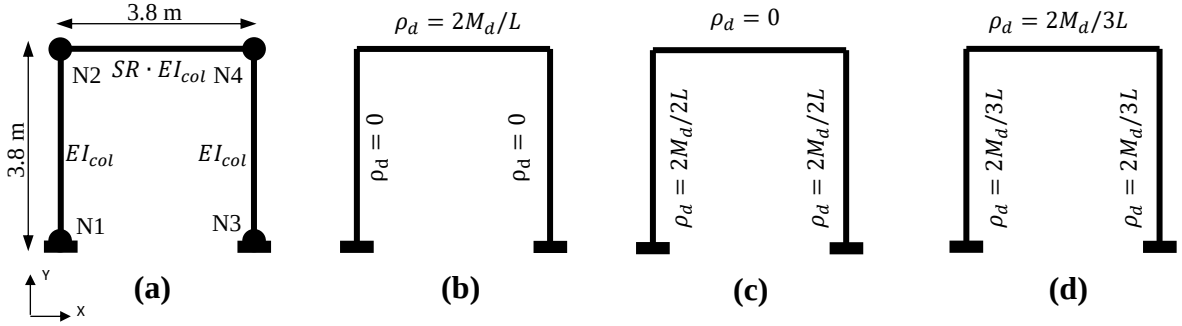

Fig. 2 – 2D frame properties used in the analyses. (a) Geometry of frame. Viscous damping distributions for (b) beam only; (c) column only, and; (d) beam-column damping.

For the purposes of this study the total damping mass M_d was taken to be equal to the total translational mass of the structure (2000kN). The total damping mass was then converted to a distributed mass by dividing by the total length of the elements contributing to the damping. The distributed damping mass applied to each of the three models is summarised in Fig. 2. The elemental viscous damping factors used in the analysis range between DF = 20 up to DF = 3000. These factors are much larger than the corresponding global viscous damping ratios. This is because the viscous damping model is no longer proportional, and the viscous damping prescribed to the element does not have the same meaning for the structure as if it were a classical model. The elemental viscous damping ratio is effectively a scale factor of the elemental viscous damping matrix that is required to produce damping forces of a magnitude that result in the desired level of global viscous damping.

For each analysis, the observed viscous damping ratio was calculated from the free vibration response using the logarithmic-decrement method [12]. This method usually only applies to systems that are classically damped, however, trial analyses showed that the decay of simple frames, damped using elemental viscous damping, matched well with the classical damping envelope across a wide range of viscous damping ratios.

2.2 Analysis results

2.2.1 Beam only damping

When the elemental viscous damping is applied only to the beam of the analysis frame, the relationship between ξ and D_F shown in Fig. 3 was obtained.

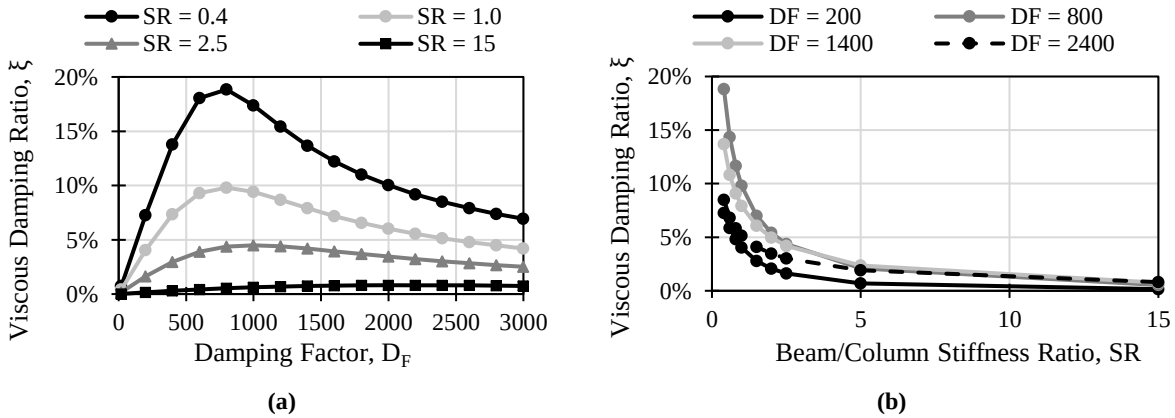

Fig. 3 – Results from the free vibration testing of simple frames with beam only damping. (a) Observed damping ratio as a function of elemental damping factor. (b) Observed damping ratio as a function of beam/column stiffness ratio.

From Fig. 3 (a) two key observations can be made. First, for a given stiffness ratio SR, the relationship between D_F and ξ is highly nonlinear. For low values of D_F, ξ increases with increasing D_F until it reaches a peak value and then it decreases asymptotically towards 0% damping. The D_F value at which the peak value of ξ occurs appears to be dependent on the stiffness ratio of the beam and columns with larger values of peak D_F corresponding to larger stiffness ratios. The second observation is that, for a given value of D_F, the stiffness ratio of the beam and columns significantly effects the level of global viscous damping observed. As the stiffness ratio increases and the beams become stiffer than the columns, the observed damping decreases. This relationship is also highly nonlinear as illustrated in Fig. 3 (b).

Note that in the case where damping is applied only to the beam elements, the assumption of axial rigid columns and beams means that there are no damping forces acting in the x-translational direction. Instead all the viscous damping is applied in the form of damping moments at nodes N2 and N4. The decrease in observed

viscous damping ratio with increasing beam/column stiffness ratio is a direct result of the decreasing rotational velocities of nodes N2 and N4.

The nonlinear relationship between the damping factor and the observed viscous damping ratio can be explained by considering the analogy of a damped tuned mass damper (TMD) like the one shown in Fig. 4 [13]. If the primary mass, M_1, of a TMD is subjected to an initial displacement and allowed to vibrate freely the relationship between the damping constant, and the observed damping ratio (Fig. 5 (a)) is very similar to the relationship between D_F and ξ that was observed in the frame tests (Fig. 3 (a)).

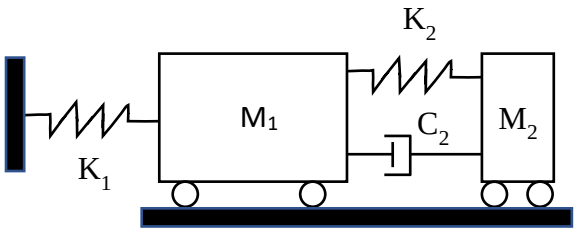

Parameter	Value
M_1	1000 kN (102 T)
M_2	100 kN (10.2 T)
K_1	50,000 kN/m
K_2	4930 kN/m
C_2	variable kNs/m

Fig. 4 – Damped tuned mass damper system

For low values of viscous damping constant, the observed viscous damping in the system is small. As the value of the damping constant increases the observed damping ratio also increases, however, if the damping constant increases above a certain level the damping ratio begins to decrease (Fig. 5 (a)). This phenomenon occurs because the damper is effectively 'locking' masses M_1 and M_2 together. These two masses then vibrate undamped on spring K_1 with almost no relative movement between them. This is evidenced by the single frequency response peak observed in highly damped TMD's (Fig. 5 (b)). A good discussion of this effect can be found in [13].

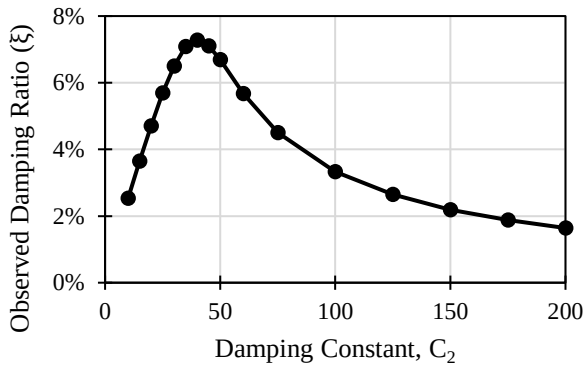

(a)

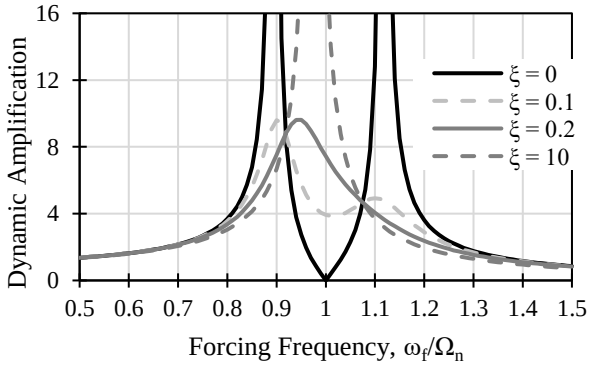

(b)

Fig. 5 – Response of the tuned mass damper system. (a) Relationship between the damping coefficient and the observed damping of the motion. (b) Frequency response function for a tuned mass damper, showing multiple damping ratios. Adapted from [13]

A similar situation occurs for the simple frame with the BO damping configuration as the damping factor, D_F, is increased. A spring and mass model analogous to the TMD model can be developed with rotational springs and dampers at N2 and N4. The damping constant of each rotational spring is proportional to the damping factor, D_F, applied to the beam. As D_F increases, the large viscous damping moments that result resist the rotation of the nodes at the end of the beam element. This causes the rotation degrees-of-freedom at

N2 and N4 to be stiffened in much the same way as the relative displacement between M_1 and M_2 of the TMD system is stiffened as C_2 increases. As discussed previously, an increase in beam stiffness, whether the result of beam geometry or increased damping, results in reduced node rotational velocities and subsequently lower damping actions and observed global damping ratios for the frame.

2.2.2 Column only damping

When the elemental viscous damping is applied only to the columns of the frame of Fig. 2 (i.e. CO damping), the relationship between ξ and D_F is significantly different to that of the BO configuration. The results from the snapback tests of the frames with CO damping are presented in Fig. 6.

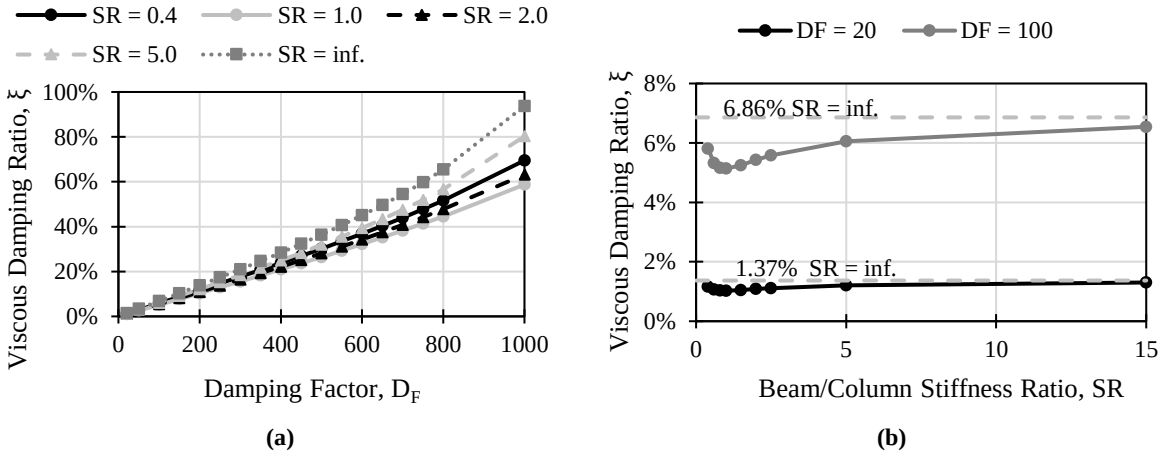

Fig. 6 – Results from the free vibration testing of simple frames with column only damping. (a) Observed viscous damping ratio as a function of elemental damping factor. (b) Variation in observed damping ratio with beam-column stiffness.

From Fig. 6 (a), key observations that can be made are: (1) For damping factors less than 500, the relationship between the damping factor and global damping ratio is almost linear; and (2) The ratio of the beam/column stiffness influences the level of global viscous damping observed. For low values of D_F, the variation in the observed viscous damping ratios is 37% ($\Delta\xi = 0.099$) across all SR values for $D_F = 500$. The variation increases significantly as D_F increases. The variation in observed viscous damping ratio is approximately 60% ($\Delta\xi = 0.35$). Curves indicating how the viscous damping ratio varies as a function of the beam/column stiffness ratio are presented in Fig. 6 (b). Unlike the beam only damping configuration, where the viscous damping ratio decreases monotonically with increasing beam/column stiffness, the effective viscous damping of the CO configuration does not. Initially, as the stiffness increases, the observed damping ratio decreases. The minimum viscous damping ratio occurs when the beam/column stiffness ratio is equal to unity. As the beams become stiffer than the columns, the viscous damping ratio increases. This behaviour can be explained by considering the two deformation modes used to define the elemental viscous damping matrix (Fig. 1). Mode one, in which the member deforms in single curvature is typical of the deformation of vibrating cantilever columns. In contrast, mode two is associated with the translation of columns deforming in shear.

When the column is stiffer than the beams, the deformations in the column tend to be dominated by mode one, but as the beam stiffness increases the deformations tend towards mode two. Mode two deformations in the columns produce both x-translational viscous damping forces and moments, unlike the beam only damping. The increasing x-velocity and the presence of an x-translational viscous damping force results in increasing observed damping ratios with increasing frame stiffness.

2.2.3 Beam and column damping

When the elemental viscous damping is applied to both the beams and columns of the analysis frame, the relationship between ξ and D_F presented in Fig. 7 (a) is obtained. Similar to the column damping model, the beam column model has a strong linear relationship between the damping factor and the observed global viscous damping ratio. A linear approximation appears to be valid for all stiffness ratios and damping factors analysed.

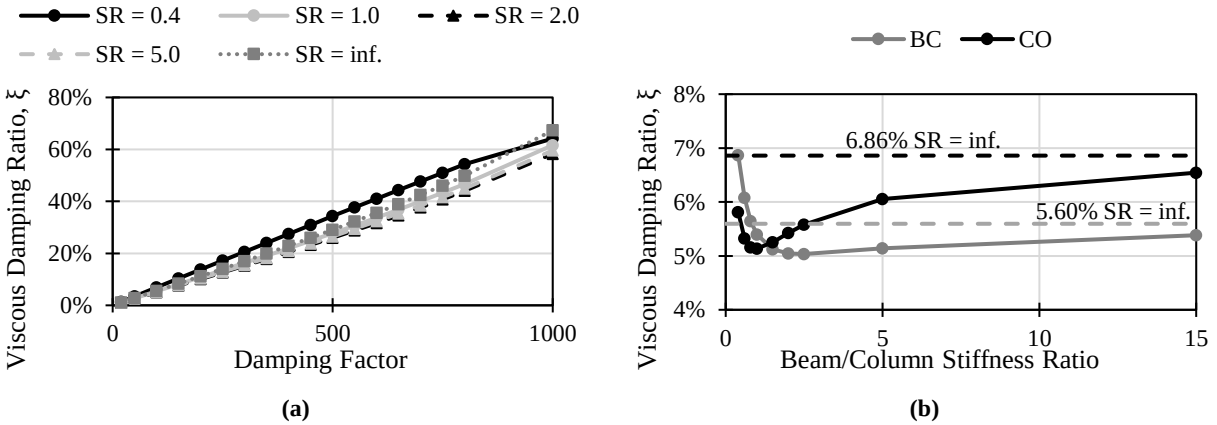

Fig. 7 – Results from the free vibration analysis of simple frames with beam-column damping. (a) Observed viscous damping ratio as a function of elemental damping factor. (b) Comparison of the variation in damping with stiffness between CO and BC damping.

As for the CO configuration, the BC configuration also exhibits a variation in the observed viscous damping ratio as a function of the beam/column stiffness ratio. Unlike the CO model, however, the variation in the viscous global damping ratio (as a percentage) decreases as the damping factor increases. The maximum variation of 36.5% ($\Delta\xi = 0.0037$) occurs for $D_F = 20$ and reduces to 24% ($\Delta\xi = 0.1040$) for $D_F = 800$.

A comparison of the damping ratios of the CO and BC models for $D_F = 100$ is presented in Fig. 7 (b). The BC model exhibits behaviour similar to the CO configuration in that the viscous damping ratio initially decreases with an increase in the beam/column stiffness ratio and then begins to increase asymptotically towards the viscous damping ratio of the rigid beam model. Although there is a clear similarity in the shape of the curves shown in Fig. 7 (b), there are substantial differences in the observed global viscous damping ratio. For stiffness ratios less than 1.5, the BC model exhibits higher levels of damping than the CO model. Additionally, the observed global damping ratio is higher than that of the corresponding rigid beam model, which is not the case for the CO configuration. For the limiting case when the beam is assumed to be rigid, the damping in the CO model is 22.5% larger than the BC model ($\xi = 6.86\%$ compared to $\xi = 5.60\%$ respectively). This is attributed to the different damping masses that were assigned to the columns in each of the models (Fig. 2).

2.3 Summary

A comparison between the $\xi - D_F$ relationships has shown that the BC and CO damping configurations are much more effective for damping the structure than the BO model. This is because these models produce a viscous damping force that acts directly on the primary translational mass, unlike the BO model that only produces viscous damping moments. In addition, the BC and CO models exhibit an almost linear relationship between the damping factor and the viscous global damping ratio. This makes it much easier to predict the

expected global viscous damping ratio given a damping factor compared to the BO model. The BC damping configuration, in general, has the lowest variation in damping ratio as a function of beam/column stiffness. This means the model can be more reliably applied to frames with different structural properties. The variation is also relatively consistent across the spectrum of damping factors analysed unlike the CO model where the variation increases rapidly for damping factors larger than 500.

3. Linear Free Vibration Analysis of Multi-storey Frame Structures

3.1 Model and analysis method

Analyses were performed on five different moment-resisting frame (MRF) structures of varying heights. Linear elastic free vibration analyses, similar to that used in Section 2, were used to investigate the relationship between the elemental viscous damping factor D_F and the observed global damping ratio ξ. Various configurations of elemental viscous damping were investigated by applying damping to; (1) the beams only, (2) the columns only, and; (3) both the beams and columns.

Five steel MRF buildings were chosen as the analysis models for this study. The frames are one, two, three, six, and nine storeys tall and are representative of realistic structures. The three, and nine storey structures are from the SAC project report, FEMA-355C [14] and designed to the 1994 edition of the Uniform Building Code (UBC) and the post-Northridge design requirements of the FEMA-267 report. The one and two-storey frames were obtained by removing the lower levels of the three-storey structure. The six-storey structure was adopted from an Earthquake Engineering Research Laboratory (EERL) study [15] and has been designed according to the 1994 UBC seismic provisions. The geometries of the analysed frames are presented in Fig. 8.

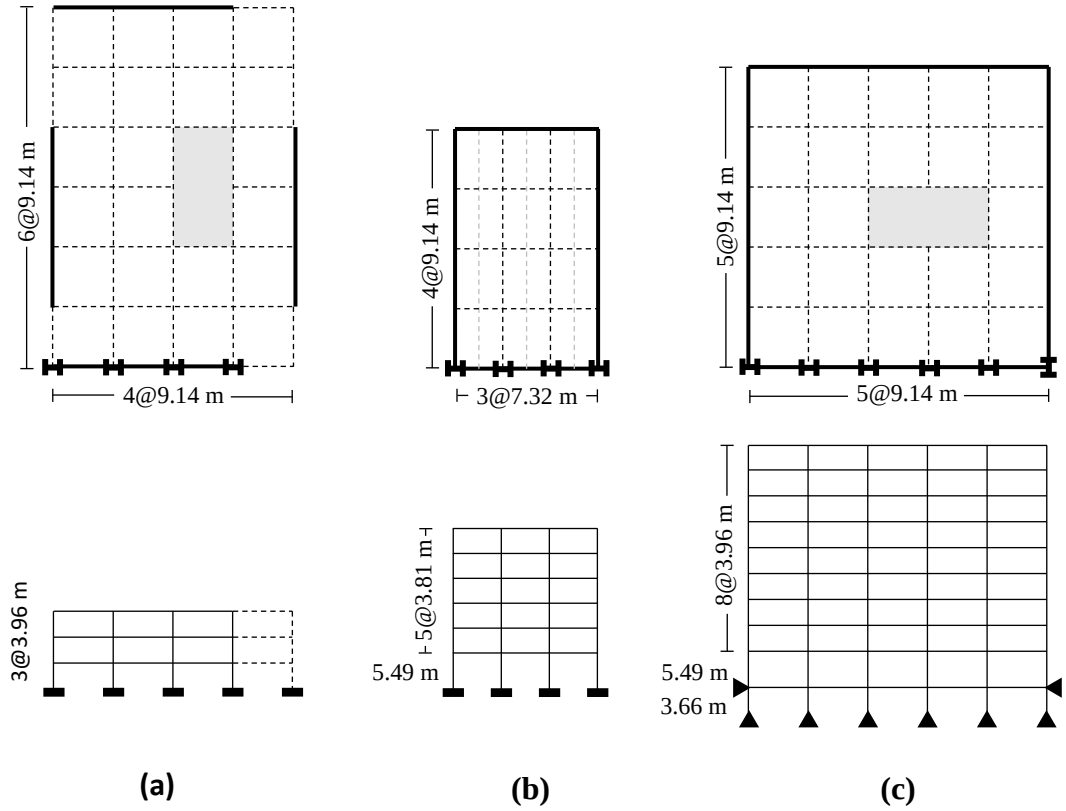

Fig. 8 - Plans and elevations of the three- (a), six- (b) and nine- (c) storey frames used in the analysis. Adapted from [14].

The buildings were analysed as 2D planar frames. All nodes at each floor were slaved to have the same horizontal translation, but free to translate vertically or rotate. Geometric P-Δ effects were accounted for using a separate leaning column that was slaved to the horizontal translation of the primary structure at each level. The seismic mass of the structure was based on the loads and floor plans provided for each frame. A lumped mass model was employed, and storey masses were lumped at the master node of each level. All analyses used a diagonal mass formulation. The beams and columns were modelled using elastic beam elements. Axial deformations of the columns were permitted. Rigid end blocks were used to model finite joint dimensions. The effects of panel zone shear deformations were modelled using zero-length rotational springs between two overlapping nodes located at each joint. The first three modal periods for each frame are presented in Table 1.

Table 1. Modal periods for the multistorey frames used in the snapback tests

	Period [s]				
Mode	**1S**	**2S**	**3S**	**6S**	**9S**
1	0.39	0.72	1.06	1.57	2.30
2	-	0.19	0.31	0.53	0.85
3	-	-	0.15	0.28	0.49

The snapback tests were performed by initially displacing each structure in its first mode shape and then releasing it to vibrate freely. The viscous damping ratio was determined using the same logarithmic decrement method as for the simple frames.

3.2 Analysis results

2.3.1 Beam only damping

The $\xi - D_F$ relationships for each of the five frame models modelled with the BO damping configuration are presented in Fig. 9 (a). From this plot, three key observations can be made: (1) within the range of damping factors considered the $\xi - D_F$ relationship is highly nonlinear for shorter structures (one-storey (1S) and two-storey (2S)) and becomes more linear as the height of the structure increases; (2) for a given damping factor the global viscous damping ratio is largest for the shorter structures, and; (3) it appears that taller structures are capable of achieving larger maximum viscous damping ratios despite producing lower damping for a given damping factor.

The nonlinear $\xi - D_F$ relationship can be attributed to the artificial stiffening of the beams that occurs in response to the presence of large viscous damping moments as discussed in Section 2.2.1. As the height of the structure increases, the damping factor at which the peak damping ratio occurs increases. This is the result of the larger frames having much longer natural periods, and therefore reduced nodal velocities. For frames with slower nodal velocities, larger damping factors are required to generate the same damping moments.

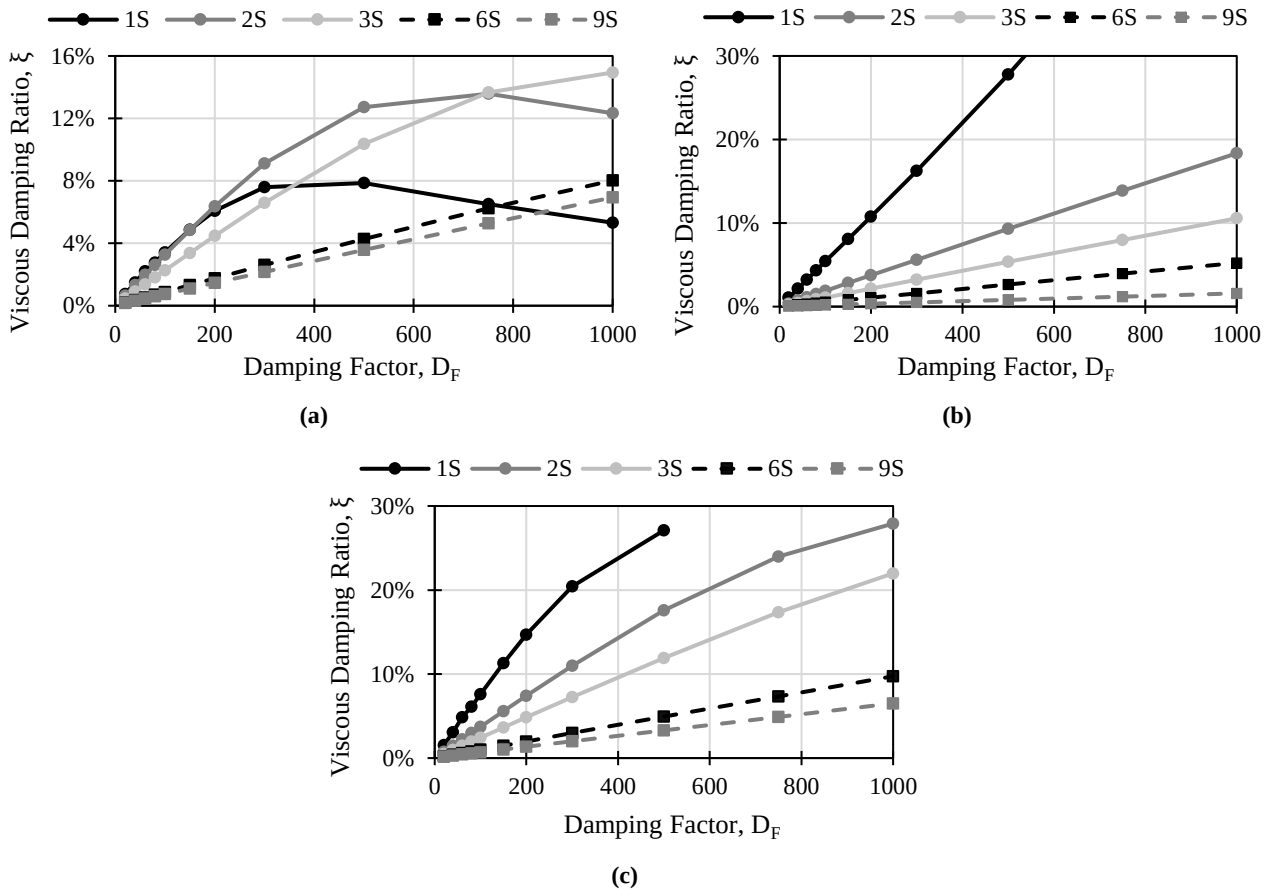

Fig. 9 – Results from the multi-storey frame analysis. (a) BO damping. (b) CO damping. (c) BC damping.

2.3.2 Column only damping

When elemental viscous damping is applied only to the columns of the analysis frames, the $\xi - D_F$ relationships shown in Fig. 9 (b) were obtained. For all the structures analysed, this relationship is strongly linear up to a damping factor of 1000. It is observed that the shorter structures exhibit much larger global viscous damping ratios (up to 60%) compared to the taller structures. The observed viscous damping ratio reduces with an increase in fundamental period and is significantly lower for all structures with two or more storeys. The CO damping model only produces a maximum of 1.6% viscous damping for the nine-storey frame even with damping factors as large as 1000. This behaviour can be explained by considering two separate issues: (1) the reduction in nodal velocities of the longer period structures; which was discussed in the previous section, and; (2) that the viscous damping is caused only by element deformations.

In all the models, the nodes at the base of the columns were fixed to resist in-plane rotation. For a given displacement, this increases the deformation of the columns in the lower storeys of the structure because there is significant relative rotation between the top and bottom of the column. In the upper storeys of the taller frames the relative rotation between the top and bottom of the column is less, so the deformations and damping forces are reduced. This is reflected in the lower viscous damping ratios observed for taller structures.

2.3.3 Beam and column damping

When damping is applied to both the beams and columns, the $\xi - D_F$ relationships presented in Fig. 9 (c) were obtained. As observed and discussed for the other damping configurations, the shorter structures, with shorter natural periods, exhibit higher viscous damping ratios than the taller structures for a given damping factor.

It is interesting to note that, for the range of damping factors considered, the $\xi - D_F$ relationship is nonlinear. This is particularly evident for the 1S structure and to a lesser degree the 2S and 3S frames. This is a markedly different result to the strong linear relationship that was observed in the simple frame tests. In Section 2, the linear relationship was attributed to the dominance of the column damping and the direct damping forces that it produces. In Fig. 9 (c), the curvature of the $\xi - D_F$ relationship is reminiscent of the response of the frames with BO damping. Possible reasons for this behaviour include the explicit modelling of panel zone flexibilities or the increased number of beams relative to the columns.

Introducing panel zone flexibility has the potential to cause the behaviour observed in Fig. 9 (c). As the damping factor increases, the viscous damping moments cause the rotations of the beams to lock, as discussed in Section 2. However, the reduced rotations at the ends of the beams are not transmitted directly to the columns because of the flexible panel zone. This means that when the beam rotations are 'locked', the column is not deforming entirely in the second (shear) mode. The relative rotation between the beam and column nodes means that as the damping actions in the beam reduce, they are not balanced by an increase in the viscous damping forces of the columns as was the case for the simple frame with no panel zone flexibility. This imbalance could result in the nonlinear relationship observed in Fig. 9 (c). Further research into the effect of flexible panel zones on the response of structures with elemental viscous damping, particularly with the BC configuration, is required to confirm this hypothesis.

3.3 Summary

The responses vary significantly depending on the damping configuration and the structure considered. The linear relationship obtained from the CO damping configuration appears to provide the most reliable relationship between the elemental viscous damping factor and the global damping ratio for the wide range of damping factors investigated. However, it is noted that the slope of the linear relationship depends strongly on the system properties and no simple relationship exists between the slope and relevant structural parameters, such as the natural period, number of stories or the number of damping elements. Although the CO damping model provides a simple relationship across a wide range of damping factors and damping ratios, it should be noted that within the range of damping ratios used in normal analysis (2-5%) the $\xi - D_F$ relationship is essentially linear for all damping models and all structures, albeit with varying slopes. The analysis results revealed that the observed damping ratio is heavily influenced by the natural period of the structure. Shorter structures, which have shorter natural periods, have increased nodal velocities and therefore result in larger damping actions and damping ratios than the taller structures. This trend was consistent across all the damping configurations.

4. Conclusion

The most important conclusion that can be drawn from this study is that the relationship between the elemental viscous damping factor, DF, and the observed global viscous damping ratio, ξ, is very complex. The analyses of the simple frames have shown that the elemental viscous damping factor required to achieve a specified level of viscous damping varied significantly depending on the structural configuration and the damping configuration used. The BO damping models exhibited a strongly nonlinear $\xi - D_F$ relationship that was significantly affected by the beam/column stiffness ratio. In contrast the CO and BC damping models exhibited almost linear $\xi - D_F$ relationships and were less sensitive to the effects of the beam/column stiffness ratio. It was shown that the BO model only generates viscous damping moments, and these were much less effective at damping the structure compared to a horizontal viscous damping force, resulting in lower peak viscous

damping ratios. It was observed that large damping factors induced a 'locking' of the joint rotations, which severely limited the effectiveness of the BO damping configuration.

From the analysis of the multi-storey frame structures it was observed that the CO damping model provided a linear relationship between the damping factor and the global viscous damping ratio. However, the slope of the relationship changed depending on the structure considered. Therefore, the damping factor required to achieve a specified viscous damping ratio depends strongly on the natural period of the structure. Longer period structures, which have lower nodal velocities, require larger damping factors to achieve a similar viscous damping ratio. This trend was consistent across all damping configurations.

5. References

[1] Lord Rayleigh (1894) *Theory of Sound – Volume 1*. Dover Publications, 2nd Edition; 1945 reissue.

[2] Wilson EL, Penzien J (1972): Evaluation of orthogonal damping matrices. *International Journal for Numerical Methods in Engineering*, **4**, 5-10.

[3] Chrisp DJ (1980): Damping models for inelastic analyses. *Master Thesis*, Department of Civil Engineering, University of Canterbury, New Zealand.

[4] Bernal D (1994): Viscous damping in inelastic structural response. *Journal of Structural Engineering*, **120** (4), 1240-1254.

[5] Charney FA (2008): Unintended consequences of modelling damping in structures. *Journal of Structural Engineering*, **134** (4), 581-592.

[6] Carr AJ (2005): Damping models in time-history structural analysis. *Asia Pacific Vibration Conference*, Langkawi, Malaysia.

[7] Chopra AK, McKenna F (2016): Modelling viscous damping in nonlinear response history analysis of buildings for earthquake excitation. *Earthquake Engineering and Structural Dynamics*, **45**, 193-211.

[8] Puthanpurayil AM, Lavan O, Carr AJ, Dhakal RP (2016): Elemental damping formulation: an alternative modelling of inherent damping in nonlinear dynamic analysis. *Bulletin of Earthquake Engineering*, **14**, 2405-2434.

[9] Carr AJ, Puthanpurayil AM, Lavan O, Dhakal RP (2017): Damping models for inelastic time-history analysis – a proposed modelling approach. *16th World Conference of Earthquake Engineering*, Santiago, Chile.

[10] Ni Y, Zhang ZY, MacRae GA, Carr, AJ, Yeow TZ (2019): Development of practical method for incorporation of elemental damping in inelastic dynamic time-history analysis. *2019 Pacific Conference on Earthquake Engineering*, Auckland, New Zealand.

[11] Carr AJ (2017): Ruaumoko3D Manual. *Report*, University of Canterbury, Christchurch, New Zealand

[12] Chopra AK (2012): *Dynamics of Structures – Theory and Applications to Earthquake Engineering.* Prentice Hall, 4th Edition

[13] Christopoulos C, Filiatrault A (2006): *Principles of Passive Supplemental Damping and Seismic Isolation*, IUSS Press.

[14] FEMA (2000): State of the art report on systems performance of steel moment resisting frames subject to earthquake ground shaking. *FEMA-335C*, Federal Emergency Management Agency, Washington DC, USA.

[15] Hall JF (1995): Parameter study of the response of moment resisting steel frame buildings to near source ground motions. *EERL 95-08*, Earthquake Engineering Research Laboratory – California Institute of Technology, Pasadena, USA.

